Surface Passivation of TiO 2 Nanowires Using a Facile Precursor-Treatment Approach for Photoelectrochemical Water Oxidation

ARTICLE *in* THE JOURNAL OF PHYSICAL CHEMISTRY C · JULY 2014

Impact Factor: 4.77 · DOI: 10.1021/jp5041019

7 AUTHORS, INCLUDING:

Ying-Chih Pu
National University of Tainan
18 PUBLICATIONS **350** CITATIONS
SEE PROFILE

Zhang Jin
Huainan Normal University
62 PUBLICATIONS **823** CITATIONS
SEE PROFILE

THE JOURNAL OF PHYSICAL CHEMISTRY C

Article

pubs.acs.org/JPCC

Surface Passivation of TiO_2 Nanowires Using a Facile Precursor-Treatment Approach for Photoelectrochemical Water Oxidation

Ying-Chih Pu,[†,‡] Yichuan Ling,[‡] Kao-Der Chang,[§] Chia-Ming Liu,[∥] Jin Z. Zhang,[‡] Yung-Jung Hsu,*[,†] and Yat Li*[,‡]

[†]Department of Materials Science and Engineering, National Chiao Tung University, 1001 University Road, Hsinchu 30010, Taiwan, ROC

[‡]Department of Chemistry and Biochemistry, University of California—Santa Cruz, Santa Cruz, California 95064, United States

[§]Mechanical and Systems Research Laboratories and [∥]Green Energy and Environment Research Laboratories, Industrial Technology Research Institute, 195, Section 4, Chung Hsing Road, Chutung, Hsinchu 31040, Taiwan, ROC

Supporting Information

ABSTRACT: We developed a facile precursor-treatment approach for effective surface passivation of rutile TiO_2 nanowire photoanode to improve its performance in photoelectrochemical (PEC) water oxidation. The approach was demonstrated by treating rutile TiO_2 nanowires with titanium precursor solutions ($TiCl_4$, $Ti(OBu)_4$, or $Ti(OiP)_4$) followed by a postannealing process, which resulted in the additional deposition of anatase TiO_2 layer on the nanowire surface. Compared to pristine TiO_2, all the precursor-treated TiO_2 nanowire electrodes exhibited a significantly enhanced photocurrent density under white light illumination. Among the three precursor-treated samples, $Ti(OBu)_4$-treated TiO_2 nanowires achieved the largest enhancement of photocurrent generation, which is approximately a 3-fold increase over pristine TiO_2. Monochromatic incident photon-to-electron conversion efficiency (IPCE) measurements showed that the improvement of PEC performance was dominated by the enhanced photoactivity of TiO_2 in the UV region. The photovoltage and electrochemical impedance spectroscopy (EIS) measurements showed that the enhanced photoactivity can be attributed to the improved charge transfer as a result of effective surface state passivation. This work demonstrates a facile, low-cost, and efficient method for preparing highly photoactive TiO_2 nanowire electrodes for PEC water oxidation. This approach could also potentially be used for other photoconversion applications, such as TiO_2 based dye-sensitized solar cells, as well as photocatalytic systems.

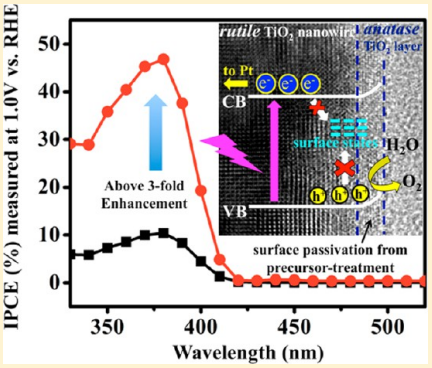

INTRODUCTION

Artificial photosynthesis for solar fuel production is a green and effective solution to development of renewable and sustainable carbon-free energy sources.[1−4] Particularly, photoelectrochemical (PEC) cells provide a promising way for practically converting solar energy to storable clean fuels such as hydrogen. Titanium dioxide (TiO_2) has been extensively utilized as photoanode in PEC water splitting because of its favorable band edge position, high chemical stability, and relatively low cost.[5−16] Under light illumination, the photogenerated holes at the valence band of TiO_2 will diffuse to the TiO_2 surface and oxidize water,[17] producing O_2. Meanwhile, the photoexcited electrons in the conduction band of TiO_2 can transfer to a (photo)cathode, reducing protons to generate H_2. The structural and surface engineering of TiO_2 photoanode is crucial to the PEC performance because charge carriers may be trapped and recombined at the surface states before they can reach the TiO_2 surface for further utilization.[18] Nanostructures with unique morphology have demonstrated desirable properties for use as highly active photoanode. For example, one-dimensional architectures, such as nanowire or nanotube arrays, have proven to be superior photoanode in PEC water splitting because the photoinduced charge carriers can easily transport to the structure surface along the radial direction.[1,19−22]

Although single-crystalline TiO_2 nanowires have a high electron mobility,[23] the photogenerated holes can be easily captured by the surface states and cause significant electron−hole recombination.[18] Atomic layer deposition (ALD) has been proved to be a powerful technique for surface state passivation to decrease trap state-mediated charge recombination.[24−26] For example, Hwang et al. demonstrated that an ALD coated TiO_2 shell on TiO_2 nanowires can increase the photocurrent by approximately 1.5 times. This improvement was attributed to the effective surface passivation of the surface states achieved by the epitaxial ALD deposition of TiO_2.[24] Similarly, Paracchino's study showed that the stability of p-Cu_2O photocathode can be substantially improved with the ALD coating of TiO_2, which prevents the self-reduction of Cu_2O.[25] Moreover, the ALD

Received: April 27, 2014
Revised: June 10, 2014
Published: June 13, 2014

   dx.doi.org/10.1021/jp5041019 | J. Phys. Chem. C 2014, 118, 15086−15094

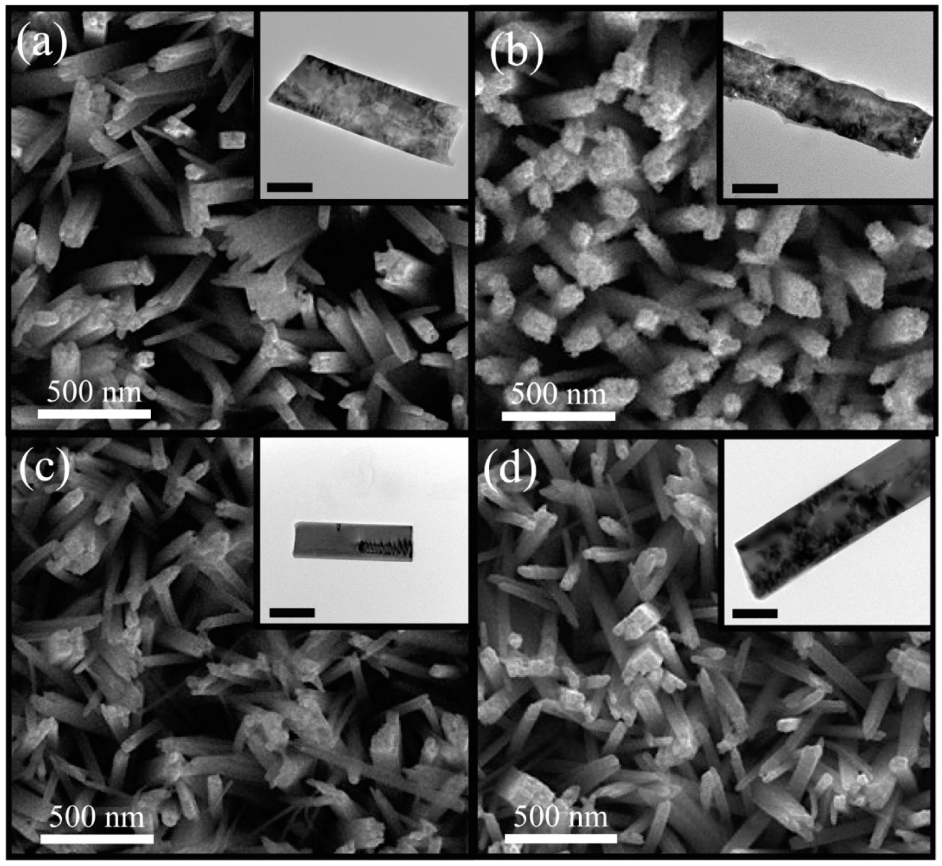

Figure 1. SEM images of (a) pristine TiO_2, (b) TiO_2-TCL, (c) TiO_2-TIP, and (d) TiO_2-TBU nanowire arrays. Insets show the corresponding TEM images of these samples. Scale bars in insets are 50 nm.

growth of p−n Fe_2O_3 has been shown to exhibit a low turn-on voltage and superior photocatalytic water splitting performance in comparison to n-Fe_2O_3. This enhancement was ascribed to the building of internal field by the p−n junction that reduces charge trapping and results in better charge separation and improved carrier utilization.[26] However, the powerful ALD technique is expensive to set up and requires hundreds of runs using layer-by-layer deposition that is time-intensive. Therefore, development of a facile wet-chemistry-based method to achieve effective surface passivation is imperative for TiO_2 electrodes. We hypothesize that the TiO_2 photoanodes can be passivated by a secondary growth of TiO_2 film using a technologically viable approach like hydrothermal process or sol−gel method.

In this work, we introduced a facile precursor-treatment approach to modify the surface of rutile TiO_2 nanowire photoanode with anatase shell and investigated its influence on the PEC water oxidation performance. Three different titanium precursors, including titanium tetrachloride ($TiCl_4$), titanium isopropoxide ($Ti(OiP)_4$), and titanium *n*-butoxide ($Ti(OBu)_4$), were employed to form anatase shells. Electron microscopy characterizations showed that a uniform layer of anatase TiO_2 film was deposited on the rutile TiO_2 nanowires after the precursor-treatment. Comparative studies demonstrated that the photocurrent of TiO_2 nanowires for PEC water oxidation can be enhanced 3-fold with the treatment of $Ti(OBu)_4$. The photovoltage measurements showed that the enhanced photoactivity of precursor-treated TiO_2 was attributable to effective surface state passivation. Furthermore, the electrochemical impedance spectroscopy (EIS) studies suggested that the significantly improved PEC performance of precursor-treated TiO_2 nanowires originates from the improved charge transfer at the TiO_2/electrolyte interface, as a result of effective surface passivation.

EXPERIMENTAL SECTION

Preparation of TiO_2 Nanowire Arrays. Rutile TiO_2 nanowire arrays were grown on fluorine-doped tin oxide (FTO) glass substrates using a hydrothermal method reported elsewhere.[6] Concentrated hydrochloric acid (15 mL) was diluted with 15 mL of deionized (DI) water and was then mixed with 0.5 mL of titanium *n*-butoxide in a 100 mL beaker. The resulting clear solution was transferred to a Teflon-lined stainless steel autoclave (40 mL volume), where a clean FTO glass substrate was submerged into the solution. The sealed autoclave was heated in an electric oven at 150 °C for 5 h and then slowly cooled to room temperature. A white TiO_2 nanowire film was uniformly coated on the FTO glass substrate after cooling. The sample was thoroughly washed with DI water and then air-dried. Finally, the sample was annealed in air at 550 °C on for 3 h to improve the crystallinity of TiO_2 nanowires.

Precursor-Treatment on TiO_2 Nanowires. Precursor-treatment of the TiO_2 nanowires was performed by using titanium tetrachloride ($TiCl_4$), titanium isopropoxide ($Ti(OiP)_4$), and titanium *n*-butoxide ($Ti(OBu)_4$) as precursors. First, the titanium precursors were dissolved in an aqueous 2 M HCl solution to form the 20% precursor sol solution. To conduct the precursor-treatment, TiO_2 nanowire arrays grown on FTO substrates were immersed in 10 mL of an aqueous HCl solution (0.025 M) containing 50 μL of the precursor

dx.doi.org/10.1021/jp5041019 | J. Phys. Chem. C 2014, 118, 15086−15094

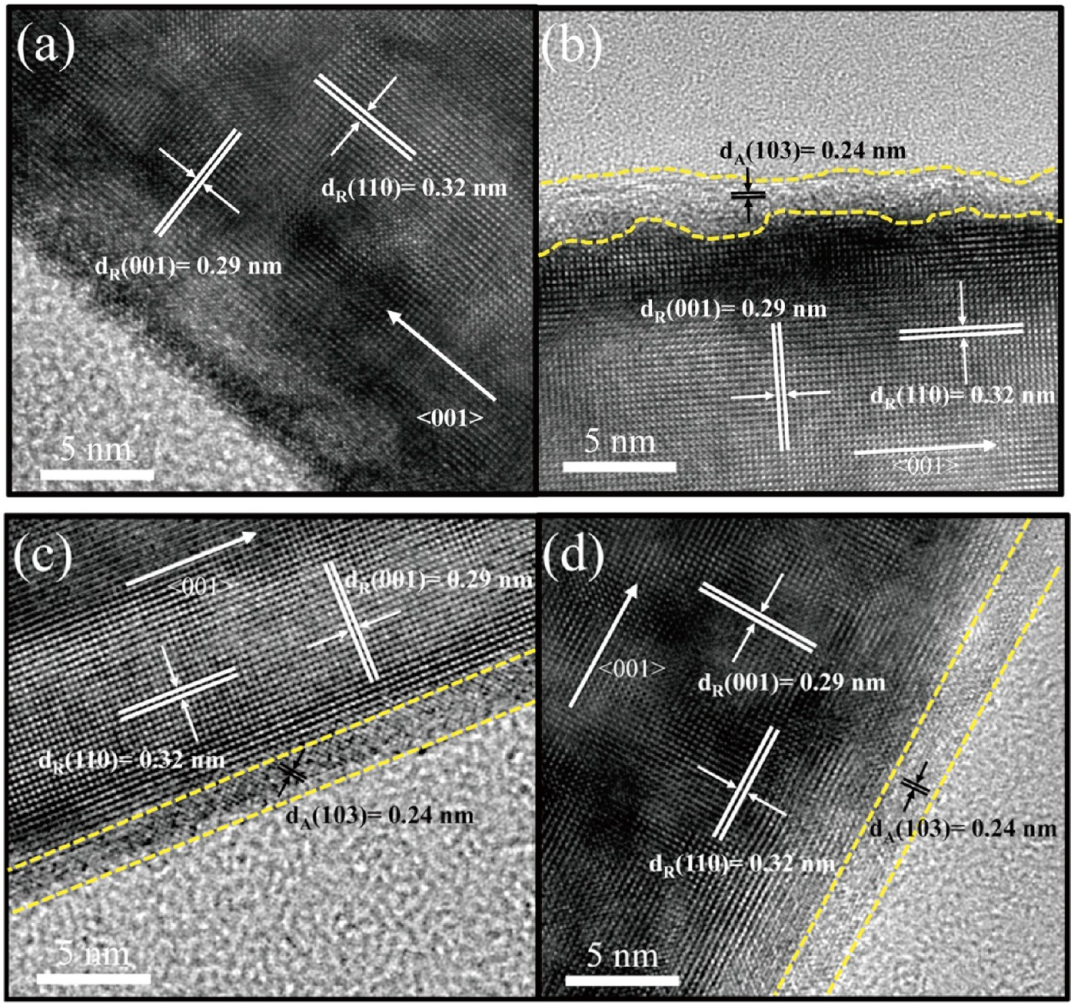

Figure 2. HR-TEM images of (a) pristine TiO_2, (b) TiO_2-TCL, (c) TiO_2-TIP, and (d) TiO_2-TBU nanowire arrays. In (b)−(d), the A-TiO_2 layers are highlighted with the inserted dashed lines.

solution in a 20 mL glass vial. The sealed glass vial was heated in an electric oven at 90 °C for 1 h and then slowly cooled to room temperature. The sample was thoroughly washed with DI water and then air-dried. Finally, the sample was annealed in air at 350 °C on a hot plate (Corning PC-420D, panel temperature was set at 550 °C) for 1 h. In this work, different amounts of $Ti(OBu)_4$ solutions (12.5, 25, 50, and 75 μL) were employed in the TBU-treatment to investigate the quantitative effect on the photoactivity of TiO_2 nanowires. The thus-obtained samples were respectively denoted as TiO_2-TBU-12.5, TiO_2-TBU-25, TiO_2-TBU-50, and TiO_2-TBU-75.

Characterization of Materials. Absorption spectra were recorded using a Hitachi U-3900H spectrophotometer at room temperature under ambient atmosphere. Scanning electron microscopy (SEM) images were collected with a field-emission SEM (Hitachi S-4800 II). Transmission electron microscopy (TEM) images were collected using a FEI monochromated F20 UT Technai TEM/STEM operated at 200 kV. X-ray diffraction (XRD) spectra were collected with Rigaku Americas Miniflex Plus powder diffractometer. Raman spectroscopy measurements were carried out on a Nicolet Almega XR dispersive Raman spectrometer (laser wavelength of 780 nm). N3/TiO_2 desorption experiments were performed using the following process. First, the prepared TiO_2 samples were immersed in a 0.3 M ethanolic solution of *cis*-bis(isothiocyanato)bis(2,2′-bipyridyl-4,4′-dicarboxylato)ruthenium(II) (N3, Fisher) for 24 h, then washed with ethanol and air-dried. After the N3/TiO_2 samples were dry, they were immersed in a solution containing 0.5 mL of ethanol and 0.5 mL of a NaOH aqueous solution (0.2 M) for 1 h to desorb the N3 dye.

Photoelectrochemical Measurements. The pristine TiO_2 and precursor-treated TiO_2 nanowire arrays were fabricated into photoanodes by soldering a copper wire onto a bare part of the FTO substrate. The substrate edges and the metal contact region were sealed with insulating epoxy resin. The working electrode area is in the range of 0.2−0.25 cm^2. A 1 M KOH aqueous solution (pH 13.6) was used as an electrolyte for PEC measurements. Linear sweeps and $I-t$ scans were measured by a CHI 660D electrochemical station using Ag/AgCl as a reference electrode and Pt wire as a counter electrode, under simulated sunlight using a 150 W xenon lamp (Newport 6255) coupled with an AM 1.5 global filter (Newport 81094). Incident-photon-to-current conversion efficiencies (IPCE) were collected by a Solartron 1280B electrochemical station with a solar simulator (Newport 69920, 1000 W xenon lamp) coupled with an infrared water filter (Oriel 6127) and aligned monochromator (Oriel Cornerstone 130 1/8 m). The EIS measurement was carried out in the frequency range from 100 kHz to 50 mHz at the open-circuit

dx.doi.org/10.1021/jp5041019 | J. Phys. Chem. C 2014, 118, 15086−15094

potential of 0.2 V. The fitting of EIS data was performed by using the Z-view software.

RESULTS AND DISCUSSION

TiO_2 nanowire arrays were synthesized on fluorine-doped tin oxide (FTO) glass substrates using a hydrothermal method reported elsewhere.[6] The prepared TiO_2 nanowires were treated with different titanium precursors by immersing them in the respective solutions at 90 °C for 1 h. The samples were then annealed in air at 350 °C on a hot plate for 1 h to increase the crystallinity. The thus-obtained TiO_2 nanowires were denoted as "TiO_2-TCL" (treated with $TiCl_4$), "TiO_2-TIP" (treated with $Ti(OiP)_4$), and "TiO_2-TBU" (treated with $Ti(OBu)_4$). The scanning electron microscopy (SEM) images shown in Figure 1 demonstrated that the morphology of the three precursor-treated nanowires is similar to that of the pristine TiO_2 nanowires. The surface characteristics of the samples were further characterized with transmission electron microscopy (TEM). As shown in the insets of Figure 1, both TiO_2-TIP and TiO_2-TBU nanowires have a smooth surface similar to pristine TiO_2. In contrast, TiO_2-TCL nanowires possess a rough surface on which a number of small particles were attached.

High-resolution TEM (HR-TEM) analysis was performed to examine the detailed structure of TiO_2 nanowires upon the precursor-treatment. As shown in Figure 2a, pristine TiO_2 nanowires exhibited a well-resolved crystalline structure with two distinct sets of lattice fringes that can be assigned to rutile TiO_2 (R-TiO_2). Compared to pristine TiO_2 nanowires that presented a homogeneous surface, all the precursor-treated samples showed atomically abrupt interfaces at the surface, suggesting that an additional layer of TiO_2 was deposited on the nanowire surface during the precursor-treatment process. The crystallographic structure of the deposited shells was identified as anatase TiO_2 (A-TiO_2) by characterizing the lattice fringes. TiO_2-TCL nanowires have a rough interface between the R-TiO_2 nanowires and A-TiO_2 shell, as revealed in Figure 2b. The thickness of the A-TiO_2 shell is approximately 1.7−2.5 nm. On the contrary, a uniform and epitaxial A-TiO_2 layer was found to form on the surface of TiO_2-TIP and TiO_2-TBU nanowires, as shown in Figure 2c and Figure 2d. The A-TiO_2 shell thickness was approximately 2 nm. In order to further confirm the crystallographic structure of TiO_2 shell, we performed the XRD and Raman characterizations for bare TiO_2 and precursor-treated TiO_2 samples. Both of the XRD and Raman analysis results indicated that the pristine TiO_2 and precursor-treated TiO_2 were rutile crystallite phase (Figure S1a and S1b in Supporting Information).[8,27] Because of the considerably small thickness, the signal contribution from the coated shell may be imperceptible in XRD and Raman measurements. In this regard, we used an indirect method to determine the structure of coated shell on TiO_2. During the precursor-treatment process, the particle suspensions are formed in the solution together with the shell coating on the TiO_2 nanowires. We annealed these particle suspensions in air at 350 °C, as we did for the core−shell nanowire samples. The XRD spectra (Figure S1c) show that the particle suspensions collected from three different precursor-treatment processes are all anatase TiO_2. These XRD results together with the TEM images suggest that the crystal phase of TiO_2 shell layers from the precursor treatment should be anatase phase. In addition, the rough surface and interface observed for TiO_2-TCL nanowires suggest that an etching process was possibly involved during the $TiCl_4$-treatment. It has been reported that Cl^- ions can easily adsorb on the (110) plane of R-TiO_2 and guide the anisotropic crystal growth to form TiO_2 nanorods because of the abundant five-coordinated Ti^{4+} atoms and oxygen vacancies.[28,29] Also, it has been demonstrated that thick R-TiO_2 nanowires could be split into secondary nanorods because of the HCl etching effect.[30,31] We postulate that the high concentration of Cl^- in the $TiCl_4$-treatment operation would enable Cl^- adsorption on the (110) plane of the R-TiO_2 nanowires, which could pose an effect analogous to HCl etching to form a rough R-TiO_2/A-TiO_2 interface. The distribution of surface roughness on the lateral (110) plane of R-TiO_2 nanowires may support the above argument.

The effect of the A-TiO_2 deposition from the precursor-treatment process on the PEC properties of TiO_2 nanowire photoanodes was studied in a three-electrode cell with a Pt wire as the counter electrode and Ag/AgCl as the reference electrode. Figure 3a shows a set of linear sweep voltammograms of pristine TiO_2 and precursor-treated TiO_2 nanowire electrodes recorded in 1 M KOH electrolyte in the dark and under white light illumination (AM 1.5G, 100 mW/cm^2). The values of potential are presented with respect to reversible hydrogen electrode (RHE), which were determined by the Nernst equation: RHE = $V_{vs\ Ag/AgCl} + E^{\circ}_{Ag/AgCl} + 0.059 \times pH = V_{vs\ Ag/AgCl} + 1.0$ V, where $E^{\circ}_{Ag/AgCl}$ is +0.1976 V at 25 °C (in 1.0 M KOH).[32] As shown in Figure 3a, the dark scans collected in the potential range between 0 and 1.5 V vs RHE displayed a negligible background current of ~10^{-8} A/cm^2. Upon light illumination, pristine TiO_2 and all precursor-treated TiO_2 nanowire electrodes showed pronounced photoresponse. Significantly, the precursor-treated TiO_2 nanowire electrodes showed higher photocurrent densities than pristine TiO_2. Among all the precursor-treated TiO_2 nanowire electrodes examined, the TiO_2-TBU electrode achieved the highest photocurrent density of 1.32 mA/cm^2 at 1.23 V vs RHE, which is almost 3 times higher than that of pristine TiO_2 (0.45 mA/cm^2) obtained at the same potential. Furthermore, the performance of surface passivated TiO_2-TBU is comparable to the best values reported for TiO_2 nanowires for photoelectrochemical water oxidation.[6,8,9,24,32,33] These results confirmed the positive role of precursor-treatment operation in enhancing the photoactivity of TiO_2 nanowires toward PEC water oxidation. This effect was further studied quantitatively. As shown in Figure S2 (Supporting Information), an optimal precursor amount for enhancing the photocurrent density of TiO_2 nanowire electrode was noticed. Overloading the amount of Ti precursor gives rise to a thick A-TiO_2 layer (Figure S3, Supporting Information). The thick A-TiO_2 layer is polycrystalline in nature and has abundant grain boundaries that may induce new trap states to obstruct hole transfer to the electrode surface. To evaluate the stability of the precursor-treated TiO_2 nanowires, an amperometric $I-t$ study was performed. The photocurrent density of TiO_2-TBU was very stable under continuous illumination for over 3 h (Figure 3b). These results demonstrated that the precursor-treated nanowires exhibited remarkable photoactivity and photostability.

To further elucidate the role of precursor-treatment operation in improving the PEC performance of TiO_2, we collected IPCE spectra for pristine TiO_2 and precursor-treated TiO_2 nanowire electrodes (Figure 3c). IPCE values at specific wavelengths can be determined from eq 1:[34]

$$\mathrm{IPCE} = (1240I)/(\lambda J_{light}) \quad (1)$$

dx.doi.org/10.1021/jp5041019 | J. Phys. Chem. C 2014, 118, 15086−15094

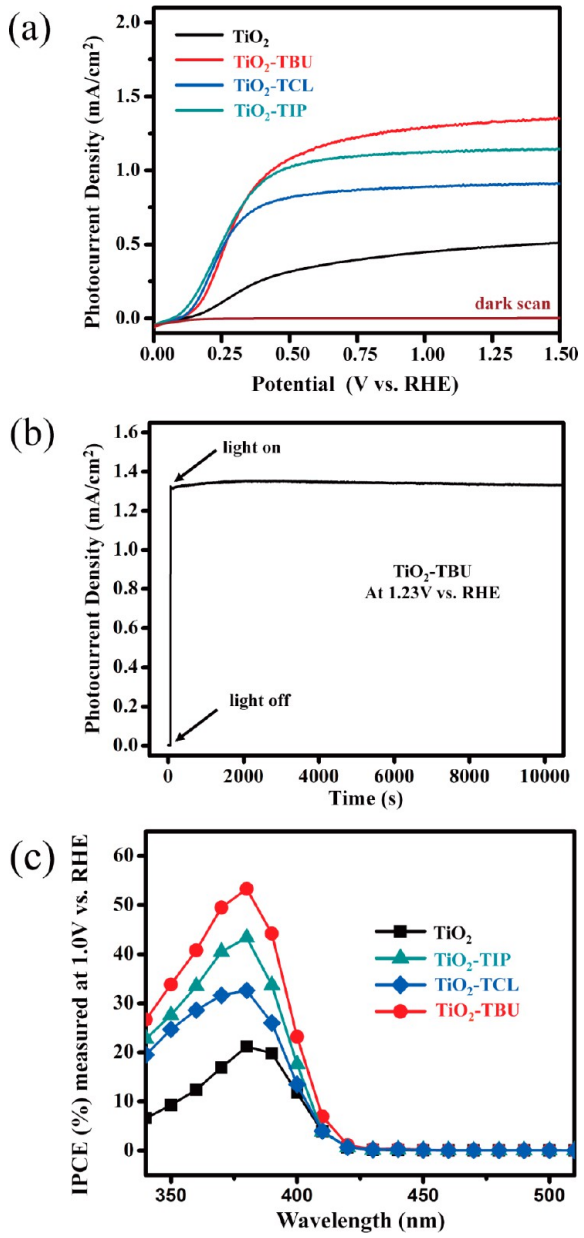

Figure 3. (a) Linear sweep voltammograms of pristine TiO_2, TiO_2-TCL, TiO_2-TIP, and TiO_2-TBU nanowire electrodes recorded in a 1 M KOH solution in the dark and under white light illumination (AM 1.5G, 100 mW/cm^2). (b) Chronoamperometric $I-t$ curve for TiO_2-TBU collected at 1.23 V vs RHE under white light illumination. (c) IPCE plots of pristine TiO_2, TiO_2-TCL, TiO_2-TIP, and TiO_2-TBU nanowire electrodes collected at 1 V vs RHE.

where I is the measured photocurrent density, J_{light} is the measured irradiance at a specific wavelength, and λ is the incident light wavelength. The precursor-treated TiO_2 nanowires exhibited higher photoactivity than pristine TiO_2 nanowires, and the TiO_2-TBU sample showed the largest IPCE enhancement. Significantly, the photocurrent enhancement of precursor-treated TiO_2 nanowires was dominated by the photoactivity of TiO_2 in the UV region, indicating that the precursor-treatment improved the water oxidation performance of TiO_2 nanowires by effectively increasing the charge collection efficiency.[35,36] Since A-TiO_2 was deposited on the surface of the precursor-treated TiO_2 nanowires, a possible cause for the improved charge collection efficiency could be the band offset created at the R-TiO_2/A-TiO_2 interface.[9] We excluded this possibility because the band alignment of R-TiO_2/A-TiO_2 in the present system was not favorable for extraction of holes. Note that the thickness of the deposited A-TiO_2 layer is around 2 nm in the precursor-treated TiO_2 samples, which could cause significant quantum effect to vary the band structure of A-TiO_2.[37] According to the effective mass approximation, a negative shift of 0.01 eV in the conduction band edge and a positive shift of 0.12 eV in the valence band edge were considered for the 2 nm thick A-TiO_2.[38,39] Although the slightly higher conduction band edge of A-TiO_2 layer may facilitate the electron transport in the R-TiO_2 nanowires, the much more positive valence band of A-TiO_2 generated an energetic barrier for hole transfer from the electrode surface to the electrolyte. Because of this unfavorable band offset, one may not expect an improved PEC performance when a 2 nm thick A-TiO_2 layer was deposited on the R-TiO_2 nanowire surface. Nevertheless, the A-TiO_2 deposition could intrinsically improve the charge collection efficiency of R-TiO_2 nanowires by considering the aspect of surface state passivation. Here we suggest that effective surface passivation is responsible for the PEC performance enhancement of precursor-treated TiO_2 nanowires.

To prove our hypothesis, we performed photovoltage and electrochemical impedance spectroscopy (EIS) measurements to evaluate the influence of A-TiO_2 on the surface properties and charge transfer at interface between photoanode and electrolyte. The surface properties of TiO_2 photoanode can significantly affect the overall PEC performance by affecting the kinetics of water oxidation as well as the charge recombination loss at electrode surface. Specifically, the photogenerated holes of TiO_2 can be trapped by the surface states and recombine with electrons before they can diffuse to the surface for water oxidation.[18] Therefore, a high density of surface trap states will negatively affect the PEC performance of TiO_2. Recent studies have demonstrated the photovoltage decay experiment as a useful method to determine the presence of surface trap states for photoanode materials.[40,41] Figure 4a shows the photovoltage−time ($V-t$) spectra for pristine TiO_2 and precursor-treated TiO_2 nanowire electrodes. Notably, all the precursor-treated TiO_2 electrodes exhibited faster photovoltage decay in comparison to the pristine TiO_2 electrode. The decay lifetime of each of the $V-t$ profiles can be determined by fitting them to the following biexponential function with two time constants (τ_1 and τ_2):

$$y(t) = A_0 + A_1 e^{-t/\tau_1} + A_2 e^{-t/\tau_2} \quad (2)$$

$$\tau_m = (\tau_1\tau_2)/(\tau_1 + \tau_2) \quad (3)$$

where τ_1 and τ_2 are time components for band-to-band and band-to-surface states charge recombination processes, τ_m is the harmonic mean of the decay lifetime, and the total half-life is $\log(2\tau_m)$. The total half-lives of pristine TiO_2, TiO_2-TCL, TiO_2-TIP, and TiO_2-TBU were estimated to be 1.25, 1.02, 0.84, and 0.72 s, respectively. The rapid decay of precursor-treated TiO_2 nanowire electrodes suggested that the precursor-treatment effectively removed the surface trap states of TiO_2 and reduced the loss of photoexcited holes via electron−hole recombination. Among the three precursor-treated TiO_2 electrodes, TiO_2-TBU showed the fastest photovoltage decay, indicating TBU-treatment rendered TiO_2 nanowires the most effective surface passivation. The trend in photovoltage decay half-life for the precursor-treated TiO_2 electrodes was in good

dx.doi.org/10.1021/jp5041019 | J. Phys. Chem. C 2014, 118, 15086−15094

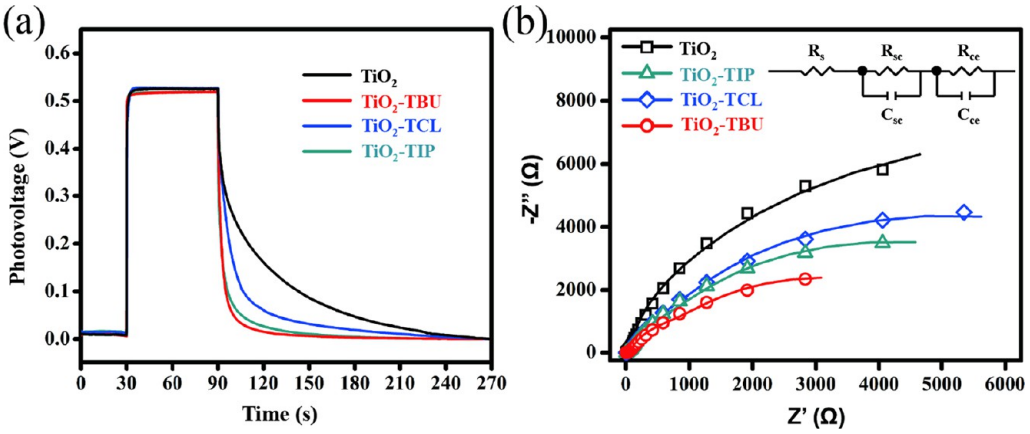

Figure 4. (a) Photovoltage–time spectra collected for pristine TiO_2, TiO_2-TCL, TiO_2-TIP, and TiO_2-TBU nanowire electrodes. (b) EIS spectra of pristine TiO_2, TiO_2-TCL, TiO_2-TIP, and TiO_2-TBU nanowire electrodes. Inset shows the equivalent circuit used to fit the spectra.

Table 1. Equivalent Circuit-Fitting Results and Kinetic Analysis for Pristine TiO_2, TiO_2-TCL, TiO_2-TIP, and TiO_2-TBU Nanowire Electrodes

	R_s (Ω)	R_{sc} (Ω)	C_{sc} (F)	R_{ce} (Ω)	C_{ce} (F)	τ_c (ms)
TiO_2	97	13.5×10^3	1.3×10^{-3}	8.8×10^2	1.7×10^{-3}	58.8
TiO_2-TCL	95	8.6×10^3	1.9×10^{-3}	8.3×10^2	1.5×10^{-3}	61.6
TiO_2-TIP	90	6.9×10^3	2.2×10^{-3}	8.1×10^2	2.1×10^{-3}	65.9
TiO_2-TBU	100	4.6×10^3	2.5×10^{-3}	8.5×10^2	1.5×10^{-3}	87.0

agreement with their IPCE results. Therefore, the photovoltage decay results supported that the enhanced photoactivity of the precursor-treated TiO_2 electrodes in PEC water splitting can be attributed to the passivation of surface trap states.

Furthermore, EIS serves as a powerful method for the study of charge transfer at the semiconductor/electrolyte interface.[42] We performed EIS measurements to investigate the influence of A-TiO_2 shell coating on the interfacial charge carrier dynamics of the TiO_2 photoanodes. Figure 4b shows the Nyquist plots of the PEC cells fabricated with pristine TiO_2 and precursor-treated TiO_2 nanowire electrodes. The impedance spectra were strongly affected by the precursor-treatment, indicating that the deposition of A-TiO_2 layer has changed the charge transfer at the electrode/electrolyte interface. The equivalent circuit[43] used to fit the EIS data was depicted in the inset of Figure 4b. In the model, R_s is the series resistance, which includes the sheet resistance of the FTO substrate and the external contact resistance of the cell. The parallel elements, R_{sc}, C_{sc}, R_{ce}, and C_{ce}, characterize the charge transfer resistance and the double layer capacitance for the TiO_2 electrode and Pt counter electrode. The fitted data for these elements are summarized in Table 1. As shown in Table 1, R_{sc} of the TiO_2 nanowire electrodes decreased after precursor-treatment. The reduction of R_{sc} indicated that the charge transfer became more efficient at the TiO_2/electrolyte interface as a result of the effective passivation of the surface trap states. Among the three types of precursor-treated TiO_2 electrodes, the TiO_2-TBU electrode showed the smallest R_{sc}, suggesting that the TBU-treatment led to the most effective surface passivation for TiO_2 nanowires. This conclusion was again consistent with the trend observed in IPCE enhancement. Furthermore, the diffusion–recombination model was used for analyzing the EIS spectra, which could estimate the lifetime of charge transfer at the interface (τ_c).[9] The characteristic time τ_c also reflects the carrier lifetime for the tested electrode. The calculated τ_c values for the pristine TiO_2 and precursor-treated TiO_2 nanowire electrodes in PEC cells were compared in Table 1. All precursor-treated TiO_2 electrodes exhibit a longer τ_c than the pristine TiO_2 electrode, which demonstrated that the precursor-treatment operation can extend the carrier lifetime of TiO_2 nanowires. The longest τ_c observed for the TiO_2-TBU electrode corresponded well with the results of IPCE and photovoltage measurements, in which TiO_2-TBU exhibited the most significantly enhanced photoactivity among all the precursor-treated TiO_2 electrodes. These results also indicate that the photoanode performance is closely related to the precursor used for forming the A-TiO_2 passivation layer. The $TiCl_4$-treatment generated a highly rough surface of TiO_2 nanowire, which could induce a high density of structural defects, causing charge recombination to shorten the carrier lifetime as observed. On the other hand, the superiority of TBU-treatment over TIP-treatment in PEC performance enhancement for TiO_2 nanowires could be attributed to the reactivity difference between the two precursors. Both TBU and TIP are typical titanium alkoxides precursor used in sol–gel synthesis of TiO_2 colloids. It has been reported that the hydrolysis and condensation rates of titanium alkoxides can be reduced as the size of alkoxy groups increases, which resulted in the formation of small colloidal clusters with more uniform size.[44,45] Since TBU has relatively larger alkoxy groups than TIP, slower hydrolysis and condensation processes are expected for the TBU-treatment, thus resulting in the slower nucleation and growth rates of the A-TiO_2. The slow A-TiO_2 deposition could relieve the formation of lattice strain at the R-TiO_2/A-TiO_2 interface, which explains why TiO_2-TBU electrode exhibited longer carrier lifetime and enhanced PEC performance compared to TiO_2-TIP.

Furthermore, the enhanced photocurrent could also be reasoned as due to the increased surface area and/or the improved light-harvesting of TiO_2 as a result of formation of the additional A-TiO_2 shell. To determine the effect of A-TiO_2 shell on surface area and light absorption of TiO_2 photoanode,

dx.doi.org/10.1021/jp5041019 | J. Phys. Chem. C 2014, 118, 15086–15094

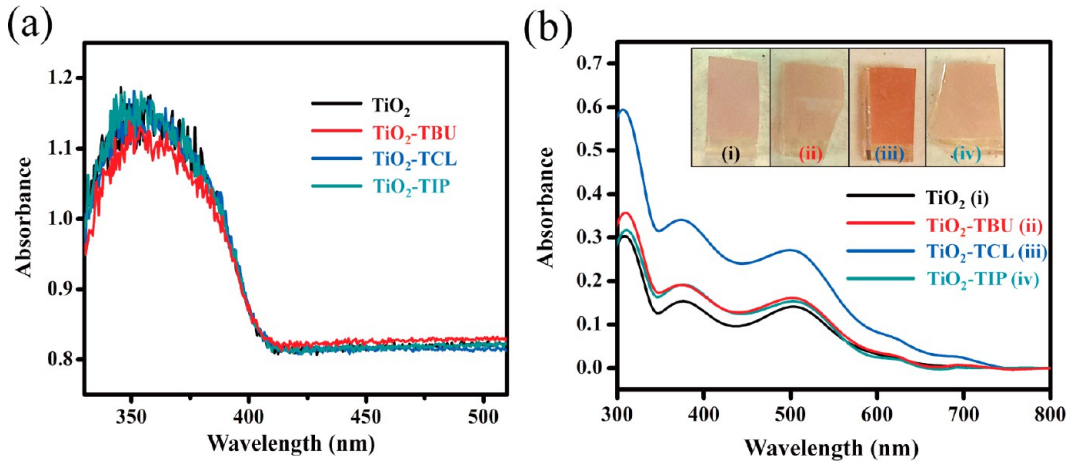

Figure 5. (a) Absorption spectra for pristine TiO_2 and precursor-treated TiO_2 nanowire array films. (b) Absorption spectra for the N3-adsorbed samples after they were immersed in a base solution for N3 desorption. Inset shows the corresponding apparent color of the samples.

the absorption spectra of the pristine TiO_2 and precursor-treated TiO_2 electrodes were collected to assess the light-harvesting ability of TiO_2. Figure 5a displays the corresponding UV−visible spectra of the samples, which showed an electronic transition from the valence band to the conduction band of TiO_2 in the UV region. Obviously, the light-harvesting ability of the TiO_2 nanowire electrode was not altered after the precursor-treatment operation. This observation ruled out the possible contribution from the increase of photon harvesting of TiO_2 upon the precursor-treatment operation. Moreover, it may also be argued that the surface area of the precursor-treated TiO_2 nanowires might have changed to account for the resultant PEC performance enhancement. To address this concern, an adsorption−desorption experiment by using N3 as the indicator dye was performed. Note that N3 dye is commonly used as a sensitizer for the TiO_2 electrode in the fabrication of DSSCs because its COOH functional group can adsorb onto the surface of the TiO_2 photoelectrode.[46] Desorption of N3 dye can easily occur when the N3-adsorbed TiO_2 electrode is immersed in a basic solution, which can be utilized to estimate the apparent surface area of a TiO_2 electrodes.[31] Figure 5b presents the UV−visible spectra for the samples after they were adsorbed by N3 and then immersed in an ethanolic solution containing NaOH. The N3-adsorption capacity of pristine TiO_2, TiO_2-TIP, and TiO_2-TBU electrodes was similar, while TiO_2-TCL exhibited higher N3 adsorption ability, which can be identified from the apparent color difference of the electrodes shown in the inset of Figure 5b. The number of adsorbed molecules (mol/cm^2) of N3 on pristine TiO_2 and precursor-treated TiO_2 nanowire electrodes can be further interpreted through the calibration absorption curve of the N3 dye. The adsorbed N3 dye on pristine TiO_2, TiO_2-TCL, TiO_2-TIP, and TiO_2-TBU electrodes were 0.039, 0.081, 0.043, and 0.045 mol/cm^2, respectively. This result signified that the apparent surface areas of the TiO_2-TIP and TiO_2-TBU electrodes were equivalent to that of the pristine TiO_2 electrode, while the TiO_2-TCL electrode with rough surface had approximately twice the surface area of the pristine TiO_2. This phenomenon further supported that the improved PEC performance of the TiO_2-TIP and TiO_2-TBU electrodes was related to effective surface passivation rather than an increase in surface area. As for the TiO_2-TCL electrode, the improved PEC performance could be partly ascribed to the surface area effect because the increase in surface area was evident.

CONCLUSION

In summary, we have demonstrated a facile, yet effective, precursor-treatment method to greatly improve the PEC properties of TiO_2 nanowires. Among the different precursor-treated TiO_2 nanowires, TiO_2-TBU showed the most significantly enhanced photoactivity and long-term stability in PEC water oxidation. The results of IPCE measurements showed that the photocurrent enhancement was mainly due to the improved photoactivity of TiO_2 in the UV region. The photovoltage and EIS results proved that the enhanced photoactivity of precursor-treated TiO_2 nanowires resulted from the effective passivation of the surface states, which suppressed trap state-mediated charge recombination to facilitate the interfacial charge transfer as well as improve the overall carrier utilization efficiency. The present precursor-treatment approach could be extended to other metal oxide electrodes for achieving effective surface passivation to enhance the overall carrier utilization efficiency. This wet-chemistry-based passivation method is economically favorable for the massive production of highly photoactive TiO_2 electrodes.

ASSOCIATED CONTENT

Supporting Information

XRD and Raman spectra; voltammograms and optimal precursor amounts for enhancing the photocurrent density of TiO_2 nanowire electrode; HR-TEM image of thick A-TiO_2 layer coated TiO_2 nanowire sample. This material is available free of charge via the Internet at http://pubs.acs.org.

AUTHOR INFORMATION

Corresponding Authors

*Y.-J.H.: e-mail, yhsu@cc.nctu.edu.tw.
*Y.L.: e-mail, yli@chemistry.ucsc.edu.

Notes

The authors declare no competing financial interest.

ACKNOWLEDGMENTS

Y.-J.H. acknowledges financial support from the National Science Council of Taiwan (Grants NSC-102-3113-P-009-002 and NSC-102-2113-M-009-005-MY2). Y.-C.P. thanks the

National Science Council of Taiwan for sponsoring the Graduate Students Study Abroad Program (Grant NSC-102-2917-I-009-042). J.Z.Z. is grateful to the BES Division of the U.S. DOE for financial support.

REFERENCES

(1) Walter, M. G.; Warren, E. L.; McKone, J. R.; Boettcher, S. W.; Santori, Q.; Mi, E. A.; Lewis, N. S. Solar Water Splitting Cells. *Chem. Rev.* **2010**, *110*, 6446−6473.
(2) Kudo, A.; Miseki, Y. Heterogeneous Photocatalyst Materials for Water Splitting. *Chem. Soc. Rev.* **2009**, *38*, 253−278.
(3) Lin, Y.; Yuan, G.; Liu, R.; Zhou, S.; Sheehan, S. W.; Wang, D. Semiconductor Nanostructure-Based Photoelectrochemical Water Splitting: A Brief Review. *Chem. Phys. Lett.* **2011**, *507*, 209−215.
(4) Liu, C.; Dasgupta, N. P.; Yang, P. Semiconductor Nanowires for Artificial Photosynthesis. *Chem. Mater.* **2014**, *26*, 415−422.
(5) Fujishima, A.; Honda, K. Electrochemical Photolysis of Water at a Semiconductor Electrode. *Nature* **1972**, *238*, 37−38.
(6) Wang, G.; Wang, H.; Ling, Y.; Tang, Y.; Yang, X.; Fitzmorris, R. C.; Wang, C.; Zhang, J. Z.; Li, Y. Hydrogen-Treated TiO_2 Nanowire Arrays for Photoelectrochemical Water Splitting. *Nano Lett.* **2011**, *11*, 3026−3033.
(7) Mohapatra, S. K.; Misra, M.; Mahajan, V. K.; Raja, K. S. Design of a Highly Efficient Photoelectrolytic Cell for Hydrogen Generation by Water Splitting: Application of $TiO_{2-x}C_x$ Nanotubes as a Photoanode and Pt/TiO_2 Nanotubes as a Cathode. *J. Phys. Chem. C* **2007**, *111*, 8677−8685.
(8) Cho, I. S.; Chen, Z.; Forman, A. J.; Kim, D. R.; Rao, P. M.; Jaramillo, T. F.; Zheng, X. Branched TiO_2 Nanorods for Photoelectrochemical Hydrogen Production. *Nano Lett.* **2011**, *11*, 4978−4984.
(9) Yang, J.-S.; Liao, W.-P.; Wu, J.-J. Morphology and Interfacial Energetics Controls for Hierarchical Anatase/Rutile TiO_2 Nanostructured Array for Efficient Photoelectrochemical Water Splitting. *ACS Appl. Mater. Interfaces* **2013**, *5*, 7425−7431.
(10) Wolcott, A.; Smith, W. A.; Kuykendall, T. R.; Zhao, Y.; Zhang, J. Z. Photoelectrochemical Water Splitting Using Dense and Aligned TiO_2 Nanorod Arrays. *Small* **2009**, *5*, 104−111.
(11) Shankar, K.; Basham, J. I.; Allam, N. K.; Varghese, O. K.; Mor, G. K.; Feng, X.; Paulose, M.; Seabold, J. A.; Choi, K.-S.; Grimes, C. A. Recent Advances in the Use of TiO_2 Nanotube and Nanowire Arrays for Oxidative Photoelectrochemistry. *J. Phys. Chem. C* **2009**, *113*, 6327−6359.
(12) Noh, S. Y.; Sun, K.; Choi, C.; Niu, M.; Yang, M.; Xu, K.; Jin, S.; Wang, D. Branched TiO_2/Si Nanostructures for Enhanced Photoelectrochemical Water Splitting. *Nano Energy* **2013**, *2*, 351−360.
(13) Palmas, S.; Polcaro, A. M.; Ruiz, J. R.; Pozzo, A. D.; Mascia, M.; Vacca, A. TiO_2 Photoanodes for Electrically Enhanced Water Splitting. *Int. J. Hydrogen Energy* **2010**, *35*, 6561−6570.
(14) Jiang, Z.; Tang, Y.; Tay, Q.; Zhang, Y.; Malyi, O. I.; Wang, D.; Deng, J.; Lai, Y.; Zhou, H.; Chen, X.; Dong, Z.; Chen, Z. Understanding the Role of Nanostructures for Efficient Hydrogen Generation on Immobilized Photocatalysts. *Adv. Energy Mater.* **2013**, *3*, 1368−1380.
(15) Xie, M.; Fu, X.; Jing, L.; Luan, P.; Feng, Y.; Fu, H. Long-Lived, Visible-Light-Excited Charge Carriers of TiO_2/ $BiVO_4$ Nanocomposites and Their Unexpected Photoactivity for Water Splitting. *Adv. Energy Mater.*, **2014**, Issue 5 (Apr 2), DOI: 10.1002/aenm.201300995.
(16) Tang, J.; Kong, B.; Wang, Y.; Xu, M.; Wang, Y.; Wu, H.; Zheng, G. Photoelectrochemical Detection of Glutathione by IrO_2−Hemin−TiO_2 Nanowire Arrays. *Nano Lett.* **2013**, *13*, 5350−5354.
(17) Grätzel, M. Photoelectrocheical Cells. *Nature* **2001**, *414*, 338−344.
(18) Leng, W. H.; Zhang, Z.; Zhang, J. Q.; Cao, C. N. Investigation of the Kinetics of a TiO_2 Photoelectrocatalytic Reaction Involving Charge Transfer and Recombination through Surface States by Electrochemical Impedance Spectroscopy. *J. Phys. Chem. B* **2005**, *109*, 15008−15023.
(19) Liu, M.; Snapp, N. d. L.; Park, H. Water Photolysis with a Cross-Linked Titanium Dioxide Nanowire Anode. *Chem. Sci.* **2011**, *2*, 80−87.
(20) van de Krol, R.; Liang, Y.; Schoonman, J. Solar Hydrogen Production with Nanostructured Metal Oxides. *J. Mater. Chem.* **2008**, *18*, 2311−2320.
(21) Kargar, A.; Sun, K.; Jing, Y.; Choi, C.; Jeong, H.; Jung, G. Y.; Jin, S.; Wang, D. 3D Branched Nanowire Photoelectrochemical Electrodes for Efficient Solar Water Splitting. *ACS Nano* **2013**, *7*, 9407−9415.
(22) Feng, X.; Shankar, K.; Varghese, O. K.; Paulose, M.; Latempa, T. J.; Grimes, C. A. Vertically Aligned Single Crystal TiO_2 Nanowire Arrays Grown Directly on Transparent Conducting Oxide Coated Glass: Synthesis Details and Applications. *Nano Lett.* **2008**, *8*, 3781−3786.
(23) Feng, X.; Zhu, K.; Frank, A. J.; Grimes, C. A.; Mallouk, T. E. Rapid Charge Transport in Dye-Sensitized Solar Cells Made from Vertically Aligned Single-Crystal Rutile TiO_2 Nanowires. *Angew. Chem., Int. Ed.* **2012**, *51*, 2727−2730.
(24) Hwang, Y. J.; Hahn, C.; Liu, B.; Yang, P. Photoelectrochemical Properties of TiO_2 Nanowire Arrays: A Study of the Dependence on Length and Atomic Layer Deposition Coating. *ACS Nano* **2012**, *6*, 5060−5069.
(25) Paracchino, A.; Laporte, V.; Sivula, K.; Grätzel, M.; Thimsen, E. Highly Active Oxide Photocathode for Photoelectrochemical Water Reduction. *Nat. Mater.* **2011**, *10*, 456−461.
(26) Lin, Y.; Xu, Y.; Mayer, M. T.; Simpson, Z. I.; McMahon, G.; Zhou, S.; Wang, D. Growth of p-Type Hematite by Atomic Layer Deposition and Its Utilization for Improved Solar Water Splitting. *J. Am. Chem. Soc.* **2012**, *134*, 5508−5511.
(27) Mali, S. S.; Betty, C. A.; Bhosale, P. N.; Patil, P. S. Hydrothermal Synthesis of Rutile TiO_2 with Hierarchical Microspheres and Their Characterization. *CrystEngComm* **2011**, *13*, 6349−6351.
(28) Hosono, E.; Fujihara, S.; Kakiuchi, K.; Imai, H. Growth of Submicrometer-Scale Rectangular Parallelepiped Rutile TiO_2 Films in Aqueous $TiCl_3$ Solutions under Hydrothermal Conditions. *J. Am. Chem. Soc.* **2004**, *126*, 7790−7791.
(29) Huang, Q.; Gao, L. A Simple Route for the Synthesis of Rutile TiO_2 Nanorods. *Chem. Lett.* **2003**, *32*, 638−639.
(30) Liu, L.; Qian, J.; Li, B.; Cui, Y.; Zhou, X.; Guo, X.; Ding, W. Fabrication of Rutile TiO_2 Tapered Nanotubes with Rectangular Cross-Sections via Anisotropic Corrosion Route. *Chem. Commun.* **2010**, *46*, 2402−2404.
(31) Lv, M.; Zheng, D.; Ye, M.; Sun, L.; Xiao, J.; Guo, W.; Lin, C. Densely Aligned Rutile TiO_2 Nanorod Arrays with High Surface Area for Efficient Dye-Sensitized Solar Cells. *Nanoscale* **2012**, *4*, 5872−5879.
(32) Wang, Y.; Zhang, Y.-Y.; Tang, J.; Wu, H.; Xu, M.; Peng, Z.; Gong, X.-G.; Zheng, G. Simultaneous Etching and Doping of TiO_2 Nanowire Arrays for Enhanced Photoelectrochemical Performance. *ACS Nano* **2013**, *7*, 9375−9383.
(33) Cho, I. S.; Logar, M.; Lee, C. H.; Cai, L.; Prinz, F. B.; Zheng, X. Rapid and Controllable Flame Reduction of TiO_2 Nanowires for Enhanced Solar Water-Splitting. *Nano Lett.* **2014**, *14*, 24−31.
(34) Wang, H.; Wang, G.; Ling, Y.; Lepert, M.; Wang, C.; Zhang, J. Z.; Li, Y. Photoelectrochemical Study of Oxygen Deficient TiO_2 Nanowire Arrays with CdS Quantum Dot Sensitization. *Nanoscale* **2012**, *4*, 1463−1466.
(35) Pesci, F. M.; Wang, G.; Klug, D. R.; Li, Y.; Cowan, A. J. Efficient Suppression of Electron−Hole Recombination in Oxygen-Deficient Hydrogen-Treated TiO_2 Nanowires for Photoelectrochemical Water Splitting. *J. Phys. Chem. C* **2013**, *117*, 25837−25844.
(36) Wang, G.; Ling, Y.; Li, Y. Oxygen-Deficient Metal Oxide Nanostructures for Photoelectrochemical Water Oxidation and Other Applications. *Nanoscale* **2012**, *4*, 6682−6691.
(37) Stroyuk, A. L.; Kryukov, A. I.; Kuchmii, S. Y.; Pokhodenko, V. D. Quantum Size Effects in Semiconductor Photocatalysis. *Theor. Exp. Chem.* **2005**, *41*, 207−228.
(38) Dresselhaus, G. Effective Mass Approximation for Excitons. *J. Phys. Chem. Solids* **1956**, *1*, 15−23.

(39) Enright, B.; Fitzmaurice, D. Spectroscopic Determination of Electron and Hole Effective Masses in a Nanocrystalline Semiconductor Film. *J. Phys. Chem.* **1996**, *100*, 1027−1035.
(40) Pu, Y.-C.; Wang, G.; Chang, K.-D.; Ling, Y.; Lin, Y.-K.; Fitzmorris, B. C.; Liu, C.-M.; Lu, X.; Tong, Y.; Zhang, J. Z.; Hsu, Y.-J.; Li, Y. Au Nanostructure-Decorated TiO_2 Nanowires Exhibiting Photoactivity across Entire UV−Visible Region for Photoelectrochemical Water Splitting. *Nano Lett.* **2013**, *13*, 3817−3823.
(41) Mukherjee, B.; Wilson, W.; Subramanian, V. R. TiO_2 Nanotube (T_NT) Surface Treatment Revisited: Implications of ZnO, $TiCl_4$, and H_2O_2 Treatment on the Photoelectrochemical Properties of T_NT and T_NT−CdSe. *Nanoscale* **2013**, *5*, 269−274.
(42) Bertoluzzi, L.; Bisquert, J. Equivalent Circuit of Electrons and Holes in Thin Semiconductor Films for Photoelectrochemical Water Splitting Applications. *J. Phys. Chem. Lett.* **2012**, *3*, 2517−2522.
(43) Lopes, T.; Andrade, L.; Ribeiro, H. A.; Mendes, A. Characterization of Photoelectrochemical Cells for Water Splitting by Electrochemical Impedance Spectroscopy. *Int. J. Hydrogen Energy* **2010**, *35*, 11601−11608.
(44) Livage, J.; Henry, M.; Sanchez, C. Sol−Gel Chemistry of Transition Metal Oxides. *Prog. Solid State Chem.* **1988**, *18*, 259−341.
(45) Wang, C.-C.; Ying, J. Y. Sol−Gel Synthesis and Hydrothermal Processing of Anatase and Rutile Titania Nanocrystals. *Chem. Mater.* **1999**, *11*, 3113−3120.
(46) Ling, Y.; Cooper, J. K.; Yang, Y.; Wang, G.; Munoz, L.; Wang, H.; Zhang, J. Z.; Li, Y. Chemically Modified Titanium Oxide Nanostructures for Dye-Sensitized Solar Cells. *Nano Energy* **2013**, *2*, 1373−1382.